THREE-DIMENSIONAL VARIABLE-DENSITY FLOW SIMULATION OF A COASTAL AQUIFER IN SOUTHERN OAHU, HAWAII, USA

Stephen B. GINGERICH (a) and **Clifford I. VOSS** (b)

(a) U. S. Geological Survey
677 Ala Moana Blvd., #415
Honolulu, Hawaii 96813 USA
(b) U.S. Geological Survey
431 National Center
Reston, Virginia 20192 USA

INTRODUCTION

Oahu Ground Water

The main population centre of the volcanic Hawaiian-island chain in the north-central Pacific Ocean is on the island of Oahu (population about 900,000) (Figure 1). Oahu depends on ground water, which is mainly produced from coastal aquifers, for its potable-water supply. Oahu has high rainfall, highly permeable aquifers, and a coastal confining layer that results in high heads at the coast and creates a very thick freshwater lens providing an ample supply of fresh ground water.

A major issue on Oahu is how much ground water can be safely produced from each aquifer without causing an unacceptable amount of saltwater intrusion. Present-day approaches to determining safe yields from the coastal aquifers are primarily based on the Ghyben-Herzberg (G-H) concept, which assumes that the depth of the middle (about 50% seawater salinity) of the transition zone (TZ) is at equilibrium with current heads in the aquifer. Although these approaches have given some insight into the behaviour of the freshwater/saltwater system, they do not effectively describe the dynamic response of the TZ to changes in pumping or rapid recharge. Most importantly, these basic approaches do not give information on the fate of the potable-water body (i.e. water fresher than 1 or 2% percent seawater), which is the primary responsibility of water managers.

The premise of the study described here is that a careful quantitative analysis of aquifer hydraulics and the physics of saltwater intrusion using state-of-the-art numerical simulation can give Oahu water managers a reliable scientific basis for deciding on water allocation and for managing Oahu's aquifer systems. The aquifer of interest in these studies is the largest Oahu aquifer, the Pearl Harbour (PH) aquifer of southern Oahu.

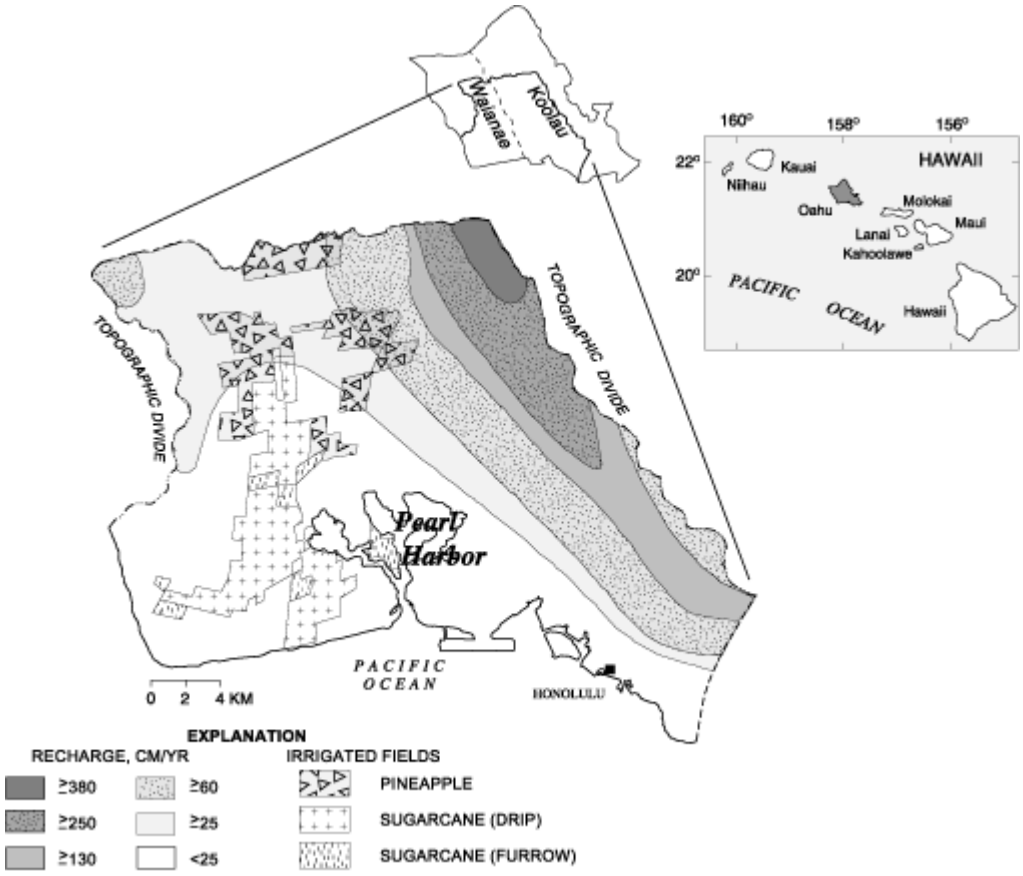

Figure 1 *Predevelopment recharge and irrigated fields, Pearl Harbour area, Oahu, Hawaii.*

The objective of this analysis is to expand a cross-sectional, two-dimensional (2D), model analysis, first published in SWIM9 proceedings (Souza and Voss, 1986; Voss and Souza, 1986), to three spatial dimensions (3D) using GIS (geographic information systems) coverages of pertinent parameters to construct the model. The approach taken in previous analyses of the PH aquifer was to apply a variable fluid density ground-water flow and solute transport code, SUTRA (Voss, 1984), to first evaluate aquifer hydraulics and then to evaluate seawater intrusion by field and numerical study of the TZ between freshwater and seawater. Subsequent work in the PH area includes: Souza and Voss (1987) and Voss and Souza (1987) (analysis of aquifer hydraulics), Souza and Voss (1989) (aquifer management), Voss and Souza (1998) (TZ dynamics), and Voss and Wood (1994) (geochemistry and ground-water ages). A summary of these works is also given in Voss (1998). A general discussion of the hydrology of Hawaii may be found in Oki and others (1997).

Hydrogeology

Oahu was built by lavas extruded from two shield volcanoes, Koolau and Waianae Volcanoes **(Figure 1)**. The bulk of the island is composed of dike-free basalts formed by sub-aerial lava flows that make up a gently dipping stratified aquifer fabric extending from land surface to considerable depth. Much of the coastal parts of the island are covered by a low-permeability sedimentary wedge (referred to as 'caprock', see Figure 3) composed of layers of marine and terrestrial sediments and clays as well as coral reef, organic debris, and volcanic deposits. The largest caprock extends offshore 30 km to 40 km south of Oahu forming a confining unit that inhibits the free discharge of fresh ground water to the ocean and the inflow of seawater to the aquifer.

The layered basalts have horizontal hydraulic-conductivity values, typically 100 to 1,000 m/d, but the stack of tabular lava-flow units may be 100 to 1,000 times less conductive vertically. The horizontal and vertical hydraulic conductivity of the caprock is 1,000 to 10,000 times less conductive than the horizontal conductivity of the layered basalt (Souza and Voss, 1987). Connected porosity, through which significant water flow can occur, is less than 10%.

Natural recharge to the PH aquifer occurs mainly in the upper-elevation areas from direct infiltration and flow from adjacent aquifer systems (Figure 1). Total predevelopment recharge to the PH aquifer was estimated to be about $1x10^6$ m^3/d (Shade and Nichols, 1996). Furrow irrigation (using surface water from eastern Oahu) of agriculture (Figure 1) began in about 1880 and was gradually phased out in the 1980's providing a source of time-varying recharge. Natural discharge from the aquifer occurs at springs at the inland caprock boundary near PH, and likely as diffuse leakage through the caprock to PH and the ocean.

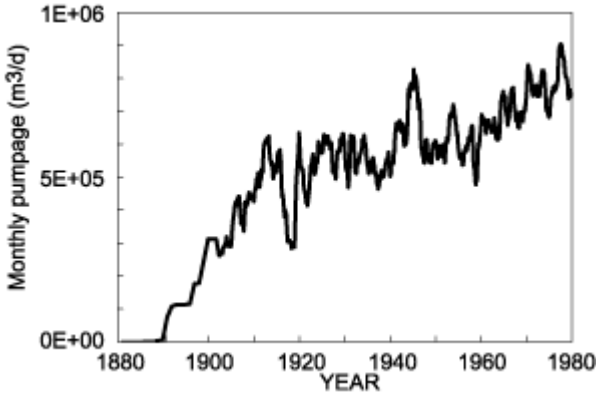

Figure 2 *Total monthly pumpage from Pearl Harbour aquifer, 1880-1980.*

Withdrawal from the aquifer began in the early 1880's, initially for sugarcane irrigation. Annual rates of withdrawal increased from the early 1900's to 1980 (Figure 2) with resultant reductions in head and upward and landward TZ movement. Most wells are located near the coast in a band that parallels the inland caprock edge (Figure 3) Over the years, some wells have been abandoned because of seawater intrusion.

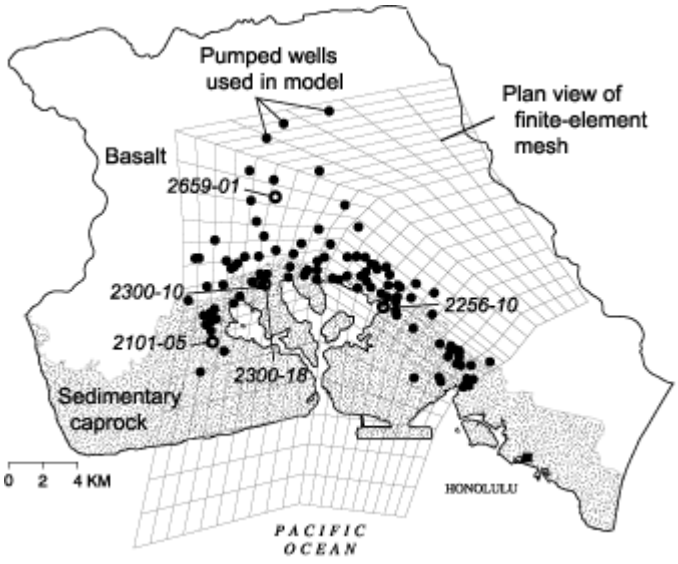

Figure 3 *Extent of sedimentary caprock, pumped (solid circles) and observation wells (open circles), and the finite-element mesh used in the ground-water model of the Pearl Harbour area, Oahu, Hawaii.*

Pre-development (pre-1880) heads in the aquifer are estimated to have been about 10 to 12 m above sea level (Mink, 1980) and thus, the pre-development freshwater-lens midpoint was 400 to 480 m deep, assuming conditions of static equilibrium with seawater. In 1990, freshwater heads ranged from about 5 to 7 m above sea level, and measured salinity profiles showed the freshwater-lens midpoint to be only 200- to 300-m deep (Voss and Wood, 1994). Thus, heads dropped 5 m from 1880 and the transition zone was reduced by about half its thickness in 100 years.

3D MODELLING

Converting 2D model to 3D model

A 3D model of the PH aquifer was developed for this study as a lateral expansion of the 2D cross-sectional model (Voss and Souza, 1986) by incorporating realistic areal distributions of hydrogeologic structure, recharge, and pumping. The objective in constructing the 3D model was to maintain the general spatial geometry and boundary conditions of the 2D cross-sectional model as well as the 2D physical property and parameter values, and to add no additional complexity except for the realistic areal geometry of model features and the extra parameters required in 3D (an additional permeability direction and five dispersivities). The 3D model is not calibrated and model simulations are mainly to demonstrate concepts and overall system behaviour.

The numerical code for the 3D model is the USGS SUTRA code, revised to include 3D as well as 2D modelling capabilities (Voss and Provost, written commun., 2002). Input data files for the 3D SUTRA model were created with the software SutraGUI (Winston and Voss, written commun., a 3D modification of Voss and others, 1997) that uses the commercial meshing-GIS software ArgusONE™. Viewing of simulation results is primarily accomplished with the software ModelViewer (Hsieh and Winston, 2002) for 3D views and SutraPlot (Souza, 1999) for line plots.

3D Model Region, Hydrogeologic Structure

The model region extends N-S about 26 km from the upstream recharge boundary to about 6 km offshore, and E-W about 22 km (Figure 3). Vertically, the model includes the entire aquifer from sea level and the sea bottom to a base at a depth of 1,800 m below sea level, the approximate depth of the low-permeability pillow basalts. The top boundary is at sea level on land and follows the sea bottom-bathymetry offshore (Figure 4). The effect of placing the top model boundary at sea level rather than at the water table is a slight underestimate (< 1%) of the transmissivity of the aquifer.

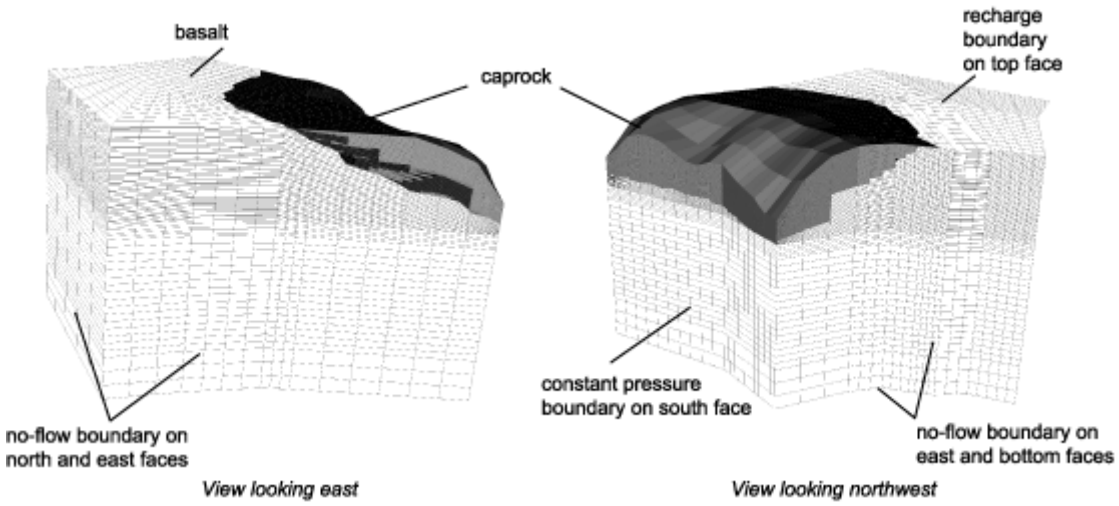

Figure 4 *Three-dimensional views of finite-element mesh used in the ground-water model of the Pearl Harbour area, Oahu, Hawaii. Ocean floor bathymetry is digitized from the USGS 1:100,000 topographic map of Oahu. The elevation of the top of the basalt beneath the caprock is based on contours digitized from Visher and Mink (1964, Figure 6) [onshore] and Gregory (1980, Figure 2) [offshore].*

Permeability is defined in two regions, the basalt, which has different vertical and horizontal permeability, and the caprock, which is assumed isotropic, although much less permeable than the basalt. Areal anisotropy and dip of major axis of the permeability tensor, aligned with the dip of the bedding, are not considered in the 3D model for the present analysis. In reality, the caprock is more complex than modelled (e.g. see Oki and others, 1998), but this analysis focuses on water in the layered basalts and a bulk representation of the caprock is used. An additional lower permeability region is defined along the entire vertical seaward boundary below the caprock to represent the resistance to saltwater inflow from and discharge to the aquifer portion that is not included in the model seaward of the boundary (Souza and Voss, 1987). Other hydraulic parameters are held constant throughout the model domain as in the 2D model. A specific yield is assigned to the part of the mesh representing the water-table surface (top of model on land), whereas compressive storage exists throughout the rest of the section.

Boundary Conditions and Recharge

Natural recharge ($1x10^6$ m^3/d; 0.0 kg-TDS/kg-fluid) enters at the water table and at the northern boundary of the aquifer (Figure 1) (Shade and Nichols, 1996), and irrigation-return recharge beneath agricultural fields is assumed constant for the period 1910 to 1980 at $0.6x10^5$ m^3/d (the 1980 value for non-caprock irrigation from Shade and Nichols, 1996). This assumption underestimates the amount of irrigation recharge in earlier decades but estimates in the form of GIS coverages of these irrigation patterns were not available.

The offshore vertical model boundaries below the sea and the top boundary below the sea are held at a pressure equivalent to the seawater depth at each node. Pressure is specified at seawater boundaries such that static equilibrium is maintained with overlying seawater allowing either seawater inflow (0.0357 kg-TDS/kg-fluid) or aquifer water outflow. The other boundaries are modelled as impermeable (no flow and no solute flux).

Observation points in the model are at locations of wells where either long-term water-level records or profiles of TZ thickness are available (Figure 3). Long-term water-level records are available at wells 2101-05 (1902-51), 2256-10 (1927-present), and 2300-10 (1910-78). TZ profiles from 1990 are available at wells 2659-01 and 2300-18.

Adjustment in model parameters for 3D model (predevelopment steady-state conditions)

Using the new 3D model with the same parameter values as the 2D model, the simulated water table was too high. The caprock hydraulic conductivity was thus increased ten-fold to 0.457 m/d in the 3D model allowing simulated water levels in the basalt aquifer to match observed water levels. The increase in caprock hydraulic conductivity is needed because of the change to the modified spatial distribution of discharge boundary conditions in the 3D model. In the 2D model, all surface nodes oceanward of the ground-surface basalt-caprock contact were held at zero pressure and the basalt-caprock contact was represented at the approximate farthest inland extent of PH. In the 3D model, PH, where much of system discharge occurs, only extends across a part of the model width. Near the inland boundary of PH, the caprock is relatively thin compared with caprock thickness along the rest of the coast. Due to the decreased lateral extent of thin caprock in the 3D model, an order-of-magnitude increase in caprock hydraulic conductivity was necessary to maintain the water-table elevation properly in the 3D model.

Simulation of aquifer response from 1880 to 1980

Transient simulation of the PH aquifer response to pumping was initiated with the hydrologic system at a pre-development steady-state condition. Withdrawal rates at each pumped well change monthly from 1880 to 1980. Because recharge and withdrawal cannot occur simultaneously in the same nodal locations in the model, all well open-interval tops are set to a maximum elevation of –6 m (i.e. 6 m below the top of the modelled land surface). All shaft wells are between –6 m and –19 m altitude. Where well open-interval data were lacking, the open interval was placed from –49 m to -99 m altitude.

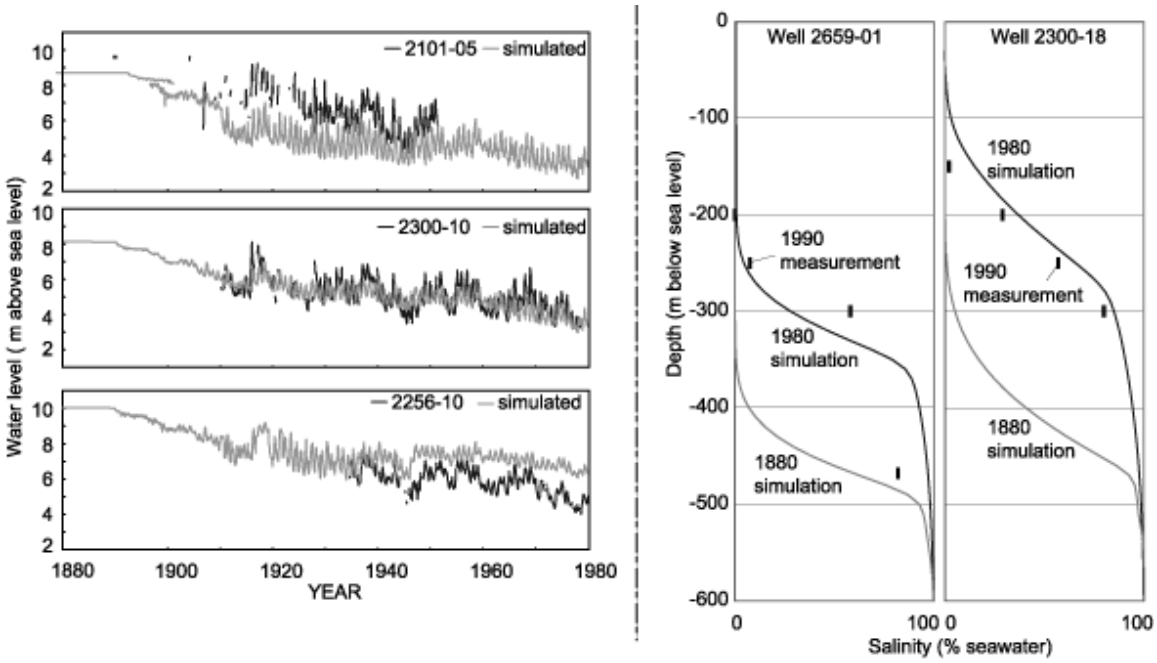

Figure 5 *Simulated water levels and salinity profiles compared with measured water levels (1880-1980) and measured salinity profiles (1990).*

The transient model reproduces the long-term water-level decrease as pumpage increases and annual water-level variations caused by seasonal pumpage variations (Figure 5). However, starting water levels in the steady-state model are too low in the west. This deviation implies that the initial 3D model does not take in to account an important unknown feature of the hydrologic system such as an east-west variation in caprock or basalt hydraulic conductivity, a major eastward-dipping unconformity, a horizontal anisotropy in basalt hydraulic conductivity, or an error in the recharge estimate.

The simulated TZ shape and position can be compared to measured values collected in 1990. Unfortunately, there are no earlier measurements of the TZ available for these wells; therefore, the predevelopment TZ is not known. At wells 2659-01 and 2300-18, the simulated midpoint is within 15 to 25 m of observed midpoint positions after 100 years of simulation (Figure 5).

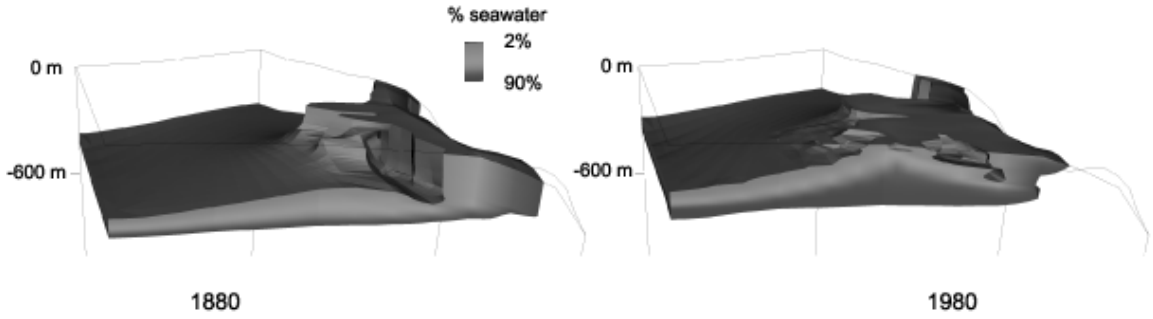

Figure 6 *3D views (looking east) of simulated transition zones, 1880 and 1980.*

Overall, from 1880 to 1980, the TZ has moved upward and thickened (Figure 6). Most thickening is in the lower half of the TZ, as found in the 2D simulations (Voss and Souza, 1998). The greatest changes are in the west where large ground-water withdrawals for irrigation also have caused the upper part of the TZ to thicken and move upward. Irrigation wells in this area gradually were abandoned throughout the 1900's due to salinity increases above unacceptable levels (Visher and Mink, 1964). Flow vectors on the water-table map show seaward-flowing ground water (Figure 7).

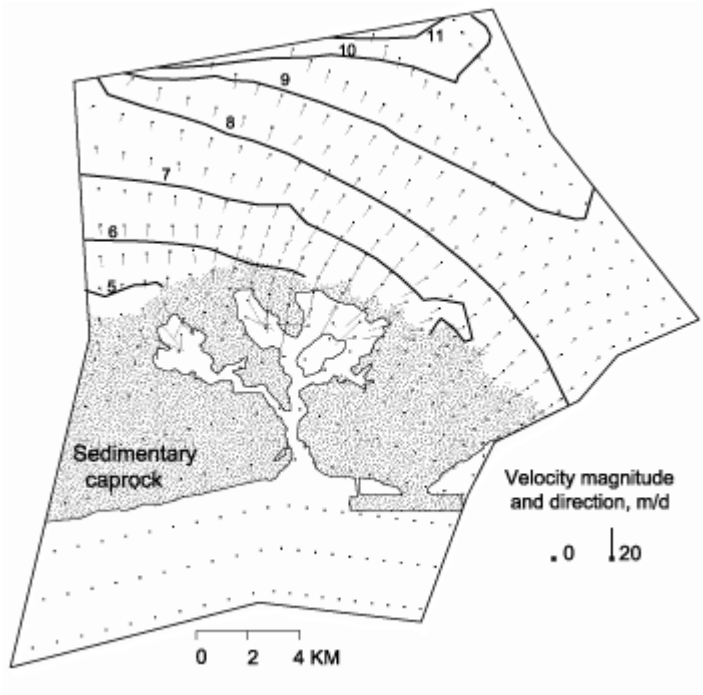

Figure 7 *Velocity vectors (projected to horizontal) at 50-m depth and simulated water-table elevation (solid contour lines in m), 1980.*

Transition-zone trends from 1880-1980 and comparison with Ghyben-Herzberg relation

One of the most useful applications of the 3D model is to simulate the TZ response to 100 years of pumping stresses. At well 2300-18, simulated trends of four salinity-concentration lines are generally parallel to each other but show more spreading below the 50% line (Figure 8). The periods of most rapid rise in the TZ near the well were between 1910-15 (5 m/yr) and 1970-75 (2.6 m/yr).

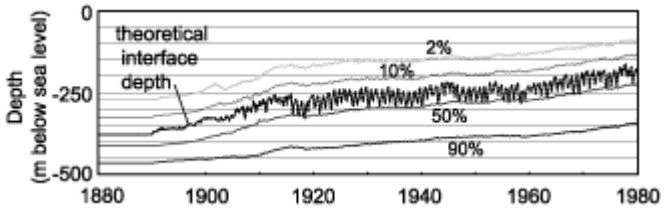

Figure 8 *Position of simulated transition zone and theoretical interface depth at well 2300-18, 1880-1980.*

In many field situations, where TZ information is lacking, the Ghyben-Herzberg relation commonly is used to estimate the TZ position and the amount of freshwater available. The relation, which assumes horizontal-flow conditions where the freshwater pressure does not change with depth, indicates that the freshwater/saltwater interface depth below sea level is 40 times the water-table elevation above sea level. The validity of this assumption can be checked by plotting the theoretical freshwater/seawater interface depth (the simulated water-table elevation multiplied by -40) on the plot showing the simulated salinity-concentration lines (Figure 8). In this simulation, the theoretical interface depth is nearly always shallower than the 50%-seawater concentration depth, indicating that the G-H relation may not be a good predictor of the TZ position. For predevelopment conditions, the theoretical interface depth was 91% of the simulated 50%-seawater concentration depth at well 2300-18. This difference can be attributed to two factors, a pressure drop in the seawater, from the ocean to the well, and a vertical freshwater-flow component. The pressure at the base of the freshwater lens in the G-H calculation is balanced against a specified pressure at the ocean boundary maintained at sea level. However, there is a pressure drop as the seawater flows landward beneath the freshwater lens

and therefore the seawater pressure balancing the lens is lower than the value assumed for the G-H relation and the freshwater lens becomes thicker than predicted by G-H. Secondly, well 2300-18 is located in a discharge zone near PH where ground-water flow has an upward component. Upward flow implies that the freshwater pressure in the TZ is higher than the freshwater pressure at the water table and an estimate of the theoretical interface depth based on the G-H relation would be too shallow using the pressure at the water table.

Throughout the 100-yr transient 3D simulation, the theoretical interface depth fluctuates between 72% and 103% of the 50%-seawater concentration depth, depending on the annual pumping stresses. The largest differences between the theoretical interface and the 50%-seawater depths occur at times of highest pumping and the closest matches followed periods of reduced pumping with associated rapid head recovery. Of more significance to groundwater management, the depth of the base of potable water (2%-seawater concentration) is as low as 41% of the theoretical interface depth from the G-H relation at well 2300-18. Therefore, the G-H theoretical interface depth is a poor predictor of the amount of potable water available in the lens. The simulations also show that annual water-table fluctuations do not translate to equivalent movement of the TZ. At well 2300-18, where annual water-table fluctuations of 1 -1.5 m would indicate theoretical interface fluctuations of 40 - 60 m, the position of the 50%-seawater isoline only fluctuates annually about 2 - 4 m, mainly because the low vertical permeability of the aquifer damps the pressure change with depth.

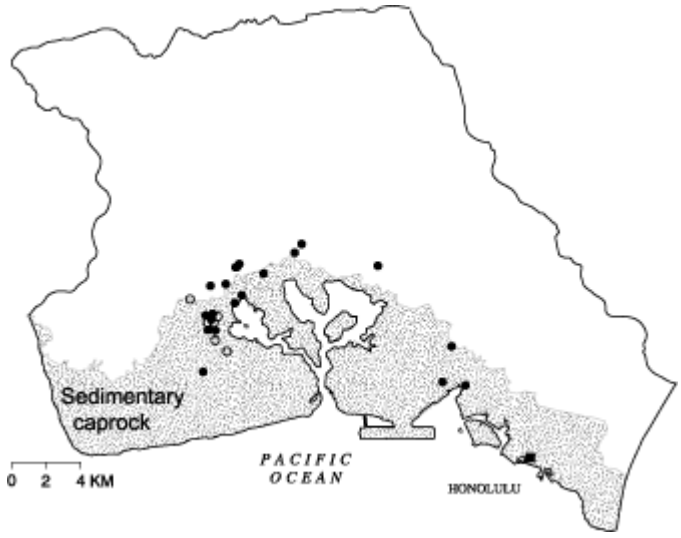

Figure 9 *Wells penetrating water with 2-percent seawater concentration at end of 1880-1980 (solid and open circles) and allocated pumping-rate (open circles) simulations.*

The 3D model also can be used to evaluate the pumping effects on the salinities at individual wells (Figure 9). Twenty-six wells penetrate water with greater than 2%-seawater concentration in the transient simulation by 1980 (withdrawal is 7.6×10^5 m^3/d). For comparison, six wells penetrate water with greater than 2%-seawater concentration after 100 years of pumping using estimated future withdrawal rates (5.5×10^5 m^3/d). Such results could be used to guide managers hoping to optimize pumping conditions in the aquifer by modifying existing infrastructure through redistributing extraction locations or by reducing the depth of the problem wells.

PARAMETER	UNITS	VALUE
General		
Freshwater density	(kg/m^{-3})	1000.
Seawater density	(kg/m^{-3})	1024.99
Water compressibility	(Pa^{-1})	$4.47x10^{-10}$
Fluid viscosity	(kg/m/s)	10^{-3}
Molecular diffusivity	(m^2/s)	$1.5x10^{-9}$
Specific yield	(1)	0.04
Aquifer matrix compressibility	(Pa^{-1})	$2.5x10^{-9}$
Caprock		
Hydraulic conductivity	(m/d)	0.457
Effective porosity	(1)	0.04
Longitudinal dispersivity, α_L	(m)	250.
Transverse dispersivity, α_T	(m)	0.25
Basalt		
Horizontal hydraulic conductivity	(m/d)	457.
Anisotropy ratio, (K_H/K_V)	(1)	200.
Effective porosity	(1)	0.04
Leakance of sea boundary	(d^{-1})	0.457
Horizontal longitudinal dispersivity, α_{LH}	(m)	250.
Vertical longitudinal dispersivity, α_{LV}	(m)	10.
Horizontal transverse dispersivity, α_{TH}	(m)	0.25
Vertical transverse dispersivity, α_{TV}	(m)	0.25

Table 1 *Parameters for Pearl Harbour model*

CONCLUSIONS

As with the 2D model upon which it is based, the 3D model reproduces the overall behaviour of ground-water flow and the freshwater/seawater TZ movement and salinity distribution in the PH aquifer. The 3D model is based on relatively simple parameterization and physics of variable-density fluid flow and solute transport. The 3D model gives results similar to that of the former 2D cross-sectional variable-density model (Voss and Souza, 1986), but it captures the spatial complexity of natural recharge, irrigation recharge, and pumping in the aquifer as well as the 3D geometry of the confining unit (caprock) and the offshore bathymetry.

The 3D model has no more parameters than the 2D model; as a result, it does not capture the E-W differences in head near PH. The trend could possibly be matched by inclusion of areal anisotropy (highest permeability parallel to direction of subareal lava flows), or by including the non-uniform permeability of the caprock. Additionally, the 3D model is missing an eastward-dipping weathered contact between basalts of different ages, which may be a low-permeability structure that reduces transmissivity of the upper aquifer from which much of the ground water is pumped. However, the 3D model approximately reproduces 100 years of historic field observations for hydraulic head and salt concentration at a number of locations during the period 1880 to 1980.

The classical G-H estimates of the depth of the freshwater/saltwater interface (40 times the head at the water table) is not a good predictor of the midpoint of the freshwater/seawater TZ, and definitely not of the potable water depth. The G-H depth occurred between about 10% and 50% seawater during the 100-year history studied. Thus, in many coastal aquifer systems, such as the PH aquifer, where the ground-water resource is being developed, the G-H depth is not the best possible parameter for coastal aquifer management. Rather, employment of a numerical simulator such as used in this analysis to predict the depth of the potable-water body as it responds to changes in hydraulic stress through time is the most effective management tool available.

REFERENCES

Gregory, A.E., III, Reflection Profiling Studies of the 500-Meter Shelf South of Oahu: Reef Development on a Mid-Oceanic Island, MS Thesis, Univ. of Hawaii, Honolulu, 1980.

Hsieh, P.A., and Winston, R.B., User's Guide to Model Viewer, A Program for Three-Dimensional Visualization of Ground-Water Model Results, U.S. Geol. Survey Open-File Rept. 02-106, 2002.

Mink, J.F., State of the Groundwater Resources of Southern Oahu, Board of Water Supply, City and County of Honolulu, 83 p., 1980.

Oki, D.S., Gingerich, S.B., and Whitehead, R.L., In Ground Water Atlas of the United States - Alaska, Hawaii, Puerto Rico and the U.S. Virgin Islands, U.S. Geol. Survey Hydrologic Investigations Atlas 730-N. --- Hawaii chapter, 1997.

Oki, D.S., Souza, W. R., Bohlke, E., and Bauer, G., "Numerical analysis of the hydrogeologic controls in a layered coastal aquifer system, Oahu, Hawaii", Hydrogeology J., **6**(2), 243-263, 1998.

Shade, P.J., and Nichols, W.D., Water Budget and the Effects of Land-Use Changes on Ground-Water Recharge, Oahu, Hawaii, U.S. Geol. Survey Prof. Paper 1412-C, 1996.

Souza, W. R., A Graphical Post-Processor for SUTRA, the U.S. Geological Survey Ground-Water Flow and Solute or Energy Transport Simulation Model, U.S. Geol. Survey Open-File Rept. 99-220, 49 p., 1999.

Souza, W. R., and Voss, C. I., "Modelling a regional aquifer containing a narrow transition between freshwater and saltwater using solute transport simulation: Part II - Analysis of a coastal aquifer system" In: Proceedings of the 9th Salt Water Intrusion Meeting, eds. Boekelman, R. H., van Dam, J. C., Evertman, M., and Ten Hoorn, W. H. C., Water Management Group, Dept. of Civil Eng., Delft Univ. of Technology, Delft, The Netherlands, 457-473, 1986.

Souza, W. R., and Voss, C. I., "Analysis of an anisotropic coastal aquifer system using variable-density flow and solute transport simulation," J. Hydrology, **92**, 17-41, 1987.

Souza, W. R., and Voss, C. I., "Assessment of potable ground water in a fresh-water lens using variable-density flow and solute transport simulation," In: Proc. National Water Well Assoc. (NWWA) Conf. on Solving Ground Water Problems with Models, Indianapolis, Indiana, 1023-1043, 1989.

Visher, F.N. and Mink, J.F., Ground-Water Resources in Southern Oahu, Hawaii, U.S. Geol. Survey Water-Supply Paper 1778, 39 p., 1964.

Voss, C. I., **SUTRA**--Saturated-Unsaturated TRAnsport--A Finite-Element Simulation Model for Saturated-Unsaturated Fluid-Density-Dependent Groundwater Flow with Energy Transport or Chemically Reactive Single-Species Solute Transport, U.S. Geol. Survey Water Res. Inv. Rept. 84-4369, 409 p. 1984,

Voss, C. I., "USGS SUTRA Code - History, Practical Use, and Application to Seawater Intrusion Modelling in Hawaii, Chapter 8," In: Seawater Intrusion in Coastal Aquifers – Concepts, Methods and Practices, eds: J. Bear, A. H-D. Cheng, I. Herrera, S. Sorek and D. Ouazar, Kluwer Academic Publishers, 249-313, 1998.

Voss, C.I., Boldt, D. and Shapiro, A.M., A Graphical-User Interface for the U.S. Geological Survey's SUTRA Code using ArgusONE (for Simulation of Saturated-Unsaturated Ground-Water Flow with Solute or Energy Transport), U.S. Geol. Survey Open-File Rept. 97-421, 106 p., 1997.

Voss, C. I., and Souza, W. R., “Modelling a regional aquifer containing a narrow transition between freshwater and saltwater using solute transport simulation: Part I - Theory and methods,” In: Proceedings of the 9th Salt Water Intrusion Meeting, eds. Boekelman, R. H., van Dam, J. C., Evertman, M., and Ten Hoorn, W. H. C., Water Management Group, Dept. of Civil Eng., Delft Univ. of Technology, Delft, The Netherlands, 493-514, 1986.

Voss, C. I., and Souza, W. R., “Variable density flow and solute transport simulation of regional aquifers containing a narrow freshwater-saltwater transition zone”, Water Resour. Res., **23**, 1851-1866, 1987.

Voss, C. I., and Souza, W. R., Dynamics of a Regional Freshwater-Saltwater Transition Zone in an Anisotropic Coastal Aquifer System, U.S. Geol Survey, Open-File Rept. 98-398, 88 p., 1998.

Voss, C. I., and Wood, W. W., “Synthesis of geochemical, isotopic and ground-water modelling analysis to explain regional flow in a coastal aquifer of southern Oahu, Hawaii,” In: Mathematical Models and their Applications to Isotope Studies in Groundwater Hydrology, International Atomic Energy Agency (IAEA) Vienna, Austria, IAEA-TECDOC-777, 147-178, 1994.